



Published in final edited form as:

Am J Sports Med. 2018 October ; 46(12): 2981–2989. doi:10.1177/0363546518793403.

A mouse model of delayed rotator cuff repair results in persistent muscle atrophy and fatty infiltration

Zili Wang, MD^{a,b,c}, Xuhui Liu, MD^{b,c}, Michael R. Davies, MD^c, Devante Horne, BS^c, Hubert Kim, MD&PhD^{b,c}, Brian T. Feeley, MD^{b,c}

^aDepartment of Orthopaedic Surgery, The Third Xiangya Hospital of Central South University, Changsha, Hunan Province, China.

^bSan Francisco Veterans Affairs Medical Center, Department of Veterans Affairs, San Francisco, CA. USA.

^cDepartment of Orthopedic Surgery, University of California at San Francisco, San Francisco, CA. USA.

Abstract

Background: Rotator cuff (RC) tears are common tendon injuries seen in orthopedic patients. Successful repair for large and massive RC tears remains a challenge due to our limited understanding of the pathophysiology of this disorder. Clinically relevant small animal models to study repair pathophysiology is limited by the lack of chronic repair models.

Purpose: To develop a highly clinically relevant delayed RC repair mouse model.

Study design: Controlled laboratory study.

Methods: Three-month-old C57BL/6J mice were underwent unilateral supraspinatus (SS) and infraspinatus (IS) tendon transection (TT) with immediate, 2-week delayed, 6-week delayed tendon repair. Animals with no repair or sham surgery served as controls. Gait analysis was conducted to measure shoulder function at 2 weeks and 6 weeks after surgery. Animals were sacrificed at 6 weeks after the last surgery. Shoulder joint, SS and IS muscles were harvested and analyzed histologically. Ex vivo mechanical testing of intact and repaired SS and IS tendons was conducted. RT-PCR was performed on SS and IS muscles to quantify atrophy, fibrosis and fatty infiltration related gene expression.

Results: Histology and tendon mechanical testing showed that torn tendons can be successfully repaired as late as 6 weeks after transection. However, significant atrophy and fatty infiltration of muscle, with impaired shoulder function was persistent in the 6-week delayed RC repair group. Shoulder function correlated with the severity of RC muscle weight loss and fatty infiltration.

Conclusions: We successfully developed a clinically relevant delayed RC repair mouse model. 6-week delayed RC repair results in persistent muscle atrophy and fatty infiltration with inferior shoulder function compared to acute repair group.

Keywords

rotator cuff tear; delayed repair; muscle atrophy; fatty infiltration; gait analysis

INTRODUCTION

Shoulder pain is the most common cause for upper extremity physician visits in the United States, ranking only behind back pain and neck pain as musculoskeletal physician visits.³⁶ Rotator cuff (RC) tears are the primary cause of persistent shoulder pain in patients.²⁹ Although some patients with RC tears remain asymptomatic, the natural history of RC tears is that they progress with an increase in symptoms and tear size over time, which eventually requires surgical repair to resume shoulder function.^{27,28,30}

The outcomes of surgery are dependent primarily on three factors: size of the tear, age of the patient, and quality of the muscle at the time of repair.^{5,11} Secondary muscle degeneration, including atrophy and fatty infiltration (FI), are critical factors that determine the clinical outcome of patients with this injury.^{3,14} It has been demonstrated that the amount of muscle atrophy and FI directly correlate with high re-tear rates and poor clinical outcomes after surgical repairs.^{6,14}

A number of small animal models are currently used to study both tendon-to-bone healing as well as muscle degeneration in the setting of RC tears and simulated repair.^{2,16,32} However, most small animal models also include a nerve injury in order to generate significant atrophy, which further limits the translatability of these models, and the majority of existing small animal RC repair models consist of tendon transection followed by immediate repair, in which the degenerative tendon and muscle changes seen in RC tears patients are absent, which limits the clinical relevance of these models. In this study, we developed a novel mouse model of delayed RC tendon repair. We evaluated tendon-to-bone healing, muscle histology, as well as shoulder function with gait analysis in mice with delayed RC tendon repairs. In our pilot study, fatty infiltration was induced at 6 weeks after tendon transection, so we chose 6 weeks as the harvest and delayed repair time point. We hypothesized that a delayed RC repair mouse model can be achieved by repairing torn SS and IS tendons at 6-week after tendon transection.

MATERIALS AND METHODS

All reagents used in this study were purchase from Fisher Scientific Corp. (Waltham, MA) unless otherwise indicated.

Surgery Procedures

One hundred and five 3-month-old female C57BL/6J mice (stock # 000664, Jackson laboratory, Sacramento, California) were used in this study. C57BL/6J mouse is a common inbred strain of laboratory mouse which is widely used as models in simulating many human diseases, including rotator cuff tears.^{2,7,18} 20 mice underwent unilateral (right side) supraspinatus (SS) and infraspinatus (IS) tendon tear (TT) without repair (5 mice for histologic staining, 5 mice for SS tendon mechanical testing, 5 mice for IS tendon

mechanical testing and 5 mice for Reverse-Transcript Polymerase Chain Reaction (RT-PCR) analysis; the same below), 20 mice underwent TT followed by immediate repair, 40 mice underwent TT and delayed tendon repair at 2 weeks (n=20) and 6 weeks (n=20) after TT, 20 mice underwent sham surgery, and the last 5 mice served as baseline controls for gait analysis (Figure 1). For the immediate repair surgery, after general anesthesia by 1–5% isoflurane, the right-side SS and IS tendons were transected as described previously.²⁵ At the time of repair, the shoulder was re-opened and remaining fibrocartilage tissue near the insertion site was then removed. Two individual 0.5-mm tunnels were created through the humerus with p-6 cutting needles (8648G, Ethicon, Somerville, New Jersey), and both tendons were fixed to their anatomical positions with 7–0 polypropylene sutures (8648G, Ethicon) (Supplement 1). Each mouse received 0.05mg/kg buprenorphine before and continuous three days after each surgery. All experiments were approved by the Institutional Animal Care and Use Committee of our institution.

Gait Analysis

DigiGait™ (Mouse Specifics Inc., Quincy, Massachusetts) analysis was conducted to measure the shoulder function at 2 weeks and 6 weeks after the final surgery as described previously.² All animals' weight were measured to confirm that there were no statistic differences among all groups before sacrificing (Data not shown). All mice walked at 10cm/s for 10s on the Digi-Gait system. Stride length, stance width, paw area at the peak stance and shared stance were chosen for the parameters to assess fore limb function. Stride length and stance width were the length and width between the central of each front paw.⁸ Paw area at the peak stance was the maximum paw area in stride.¹⁷ The three parameters indicated the pain and ability of loading the limb. Share stance was the percent of stance that the two hind paws touch the track simultaneously, indicating the weakness of fore limb function.

Muscular Harvesting and Wet Muscle Weight

All Mice were sacrificed at 6 weeks after last surgery. For assessing muscle atrophy, wet weight of bilateral SS and IS muscles were measured immediately after harvesting. The percent change of wet muscle weight was measured using the following evaluation: $([SS_{Right} - SS_{Left}] / SS_{Left}) \times 100\%$ and $([IS_{Right} - IS_{Left}] / IS_{Left}) \times 100\%$.¹⁰

Histology

SS (N=5 per group) and IS (N=5 per group) muscles were mounted on cork disks with 10% w/v tragacanth gum (Sigma-Aldrich, St. Louis, Missouri) in water and then flash-frozen in liquid nitrogen-cooled 2-methylbutane and then cryosectioned at a thickness of 10 μm .²⁵ Masson trichrome (American MasterTech, Lodi, California) and oil red-O (Sigma) staining were used to assess the fibrosis and fatty infiltration in SS and IS muscles. Shoulder joints were fixed overnight in 4% paraformaldehyde and decalcified for 2 weeks in 10% EDTA. After dehydrating in grading ethyl alcohol and xylene, samples were embedded in paraffin and then sectioned at a thickness of 5- μm . Hematoxylin and eosin (H & E) staining was performed to assess the morphology of both SS and IS tendon. Slides were covered with 10% glycerol in PBS (for Oil red-O) or 50% resinene in xylene (for H & E and Masson trichrome) and observed on an optical microscope (Axio Imager; Zeiss).

Pictures were analyzed using ImageJ (National Institutes of Health). Cross sections were chosen randomly from mid-bellies of SS and IS. All pictures were assessed by two blinded researchers. Cross sections area was measured by for muscle fibers in five randomly selected areas on sections from mid-bellies of SS and IS muscles. 600 to 2000 fibers in each sample were calculated. The area fraction of collagen was calculated by dividing the area of Aniline Blue staining by the entire sample area. Similarly, the area fraction of fat was assessed by dividing the area of ORO staining by the entire sample area. The images were measured by the two observers, and the average value was calculated for each sample as described previously.²⁵

Tendon Mechanical Testing

The initial cross-sectional area (CSA = thickness × width) and length of tendon was measured with a custom laser device.³³ Intact, un-repaired, and repaired SS and IS tendons were subjected to uniaxial tensile tests to failure using a mechanical loading frame (ElectroForce 3200; Bose, Eden Prairie, MN). SS or IS muscle was glued between narrow strips of sandpaper with cyanoacrylate (Loctite Super Glue Gel Control) as the bonding agent. The sandpaper was gripped with a custom grip, and the humerus was potted in smooth cast mixture (Smooth-on INC., Macungie, Pennsylvania). The humerus was held at about 30° angle (for SS) or 90° angle (for IS) to ensure the tendons are parallel to the actuator. For IS tendon, to hold the humerus horizontally when potting, a custom post was designed using SolidWorks (Dassault Systèmes, Waltham, MA) and then printed with a 3D printer (Flashforge, Los Angeles, CA) using poly-lactic-acid filament (Filaments.CA, Toronto, ON). To provide each specimen a uniform strain history before loading, each was preconditioned for 6 oscillation cycles at 1Hz between 0 and 1mm displacement. Specimens were vertically stretched using a linear ramp loading profile at a strain rate of 0.03mm/s. Vertical force and displacement was recorded in real-time, and ramping was terminated after failure, indicated by a 1.5N drop in force. Then, Maximum Load, displacement, stiffness, strength and the location of rupture were measured for each sample as described previously.³⁴

RT-PCR

RT-PCR was performed to examine the muscle atrophy (Atrogin-1, MuRF-1),^{13,24,26} fibrosis (α-SMA, Collagen-1a, Collagen-3a)^{23,26} and FI (PPAR-g1, PPAR-g2, c/EBP-a, ADIPOQ)^{4,15,26} related gene expression in the RC muscles. Total RNA for both SS (N=5 per group) and IS (N=5 per group) was extracted using Trizol reagent according to the instructions. Transcriptor First Strand cDNA Synthesis Kit (Roche Applied Bioscience Inc., Indianapolis, IN.) was applied to synthesize cDNA. RT-PCR was performed to quantify gene expression of using SYBR Green Detection and an Applied Biosystems Prism 7900HT detection system (Applied Biosystems, Inc., Foster City, CA). Sequences of the primers for target genes were showed in Supplement 2. The expression level of each gene was normalized to that of the house-keeping gene of S26. S26 is a common house-keeping gene that express stably in mouse muscle. Fold changes relative to sham controls were calculated by CT.

Statistical Analysis

Analyses of variance (ANOVA) with Tukey post hoc comparisons were used to calculate difference in the percent wet muscle weight change, area fraction of collagen, area fraction of fat and gene expression among all groups. For the 6-week delayed repair group, Pearson correlation coefficient was used to evaluate the correlation between the functional data (gait analysis) and the muscle/tendon data (percent wet muscle weight change, fat area fraction in muscle or tendon mechanical testing). Statistical significance was set at $P < .05$.

RESULTS

Tendon Histological Assessment

H&E staining showed that SS and IS tendons were reattached to humeral head in immediate repair, 2-week and 6-week delayed repair groups. Although more synovial tissue proliferation and unorganized tendon was found in the 2 delayed repair groups when compared to the immediate group, there was no gapping in the tendon from the suture hole to the humeral head cartilage for all samples from the three repair groups. However, in TT group, only loose scar tissue was seen between the torn tendons and humeral head (Figure 2).

Muscle Atrophy, Fibrosis and Fatty Infiltration

The TT group and the 6-week delayed group had significantly more muscle weight loss and smaller muscle fiber cross-sectional area compared to the sham group, the immediate group and the 2-week delayed repair group ($P < .05$). No statistical differences were found among the sham group, the immediate, and the 2-week delayed repair groups ($P > .05$) (Figure 3). Masson trichrome and oil red-O staining demonstrated significantly more fibrosis and fatty infiltration in SS and IS muscles from the TT group and the 6-week delayed repair group, with only minimal fibrosis and fatty infiltration seen in immediate group and the 2-week delayed repair group (Figure 4).

Mechanical Testing

Mechanical testing demonstrated that mechanical properties (max load, stiffness and strength) of SS and IS tendons from the TT group were significantly inferior to those in the other four groups ($P < .05$). No differences were found among the three repair groups ($P > .05$). In addition, all tendons from the TT group failed at the junction between the scar and the humeral head. However, the majority of failure locations for the tendons from the sham group and the three repair groups occurred in the tendon-muscle junction, indicating that both SS and IS tendons were well healed to the insertion site on the humeral head. (Table 1).

Gait Analysis

DigiGait™ analysis exhibited abnormal upper limb gait at surgery side in animals from all surgery groups (except for sham) at 2 weeks after the last surgery. At 6 weeks, although other groups recovered, shoulder function in the TT and the 6-week delayed repair group remained inferior the control group ($P < .05$) (Figure 5). Correlation coefficient analysis showed no significant correlations between mechanical properties of SS (or IS) tendon and

gait analysis. However, both percent wet muscle weight change and fat area fraction showed significant correlation to stride length, stance width and paw area at peak stance (Table 2), suggesting that muscle quality was a primary factor in surgical outcome in these groups.

Gene Expression

Atrophy, fibrosis and fatty infiltration-related gene expression was significantly up-regulated in the TT group (3.0–4.0 fold, respect to the sham) and the 6-week delayed repair group (2.0–3.5 fold, respect to the sham), while no significant differences were found in the immediate repair group and the 2-week delayed repair group (Figure 6).

DISCUSSION

Chronic RC tears lead to degeneration of the cuff muscles with atrophy and fatty infiltration increasing with the size of the tear. This is seen in populations with anterior rotator cable tears as well as patients with large and massive tears: rotator cuff muscles often show marked muscle atrophy and fatty infiltration observed by both computed tomography and magnetic resonance imaging (MRI) and on visual inspection at the time of surgical intervention.²⁰ In the present study, muscle atrophy after chronic tendon tears was verified by wet weight loss and reduction of muscle fiber cross-section area histologically. Muscle fatty infiltration was verified with histological analysis with oil red o fat staining. Histological findings of muscle atrophy and fatty infiltration, which was proven to be highly correlated to MRI analysis in our mouse model,³⁵ is supported by significantly increased expression of atrophy, fibrosis and fatty infiltration related genes as measured with RT-PCR at 6 weeks after tendon transection. These data suggests that muscle atrophy and fatty infiltration at 6 weeks after tendon transection represents muscle degeneration seen in chronic RC tear patients clinically. Thus, we believe a delayed repair at 6 weeks after tendon transection represents tendon repair in chronic RC tear patients clinically.

In this study, we developed a novel, clinically relevant mouse model of delayed RC tendon repair. Though torn supraspinatus and infraspinatus tendons can be successfully repaired as late as 6 weeks after transection, muscle atrophy and fatty infiltration of muscles with impaired shoulder function persisted even after successful tendon repair, similar to what is seen clinically in many patients. This model will allow for the study of cellular and molecular changes after RC repair, the use of genetically manipulated animals to study these changes, and an avenue to study pharmacologic and cellular therapies to improve healing in chronic RC injury.

Similar to other fields in orthopedics, animal models are powerful tools for study human RC tear pathogenesis and treatments. RC tear models have been successfully developed in mouse, rat, rabbit, dog, sheep/goat and nonhuman primates.^{9,21} However, few RC repair models are available at present, and most are in larger animals, or involve acute repairs. Bell et al. reported a mouse model of immediate post-transection repair of supraspinatus tendon.² Kovacevic and his colleagues have reported rat rotator cuff acute repair model.¹⁹ Delayed rotator cuff repair models have only been only reported in rabbit²² and sheep.¹² Because degenerative tendon pathology and muscle atrophy/fatty infiltration only exist in chronic RC tears, delayed repair models have significantly higher clinical relevance compared to acute

repair models. Though larger animals may have similar size (but not necessarily anatomy) of RCs when compared to humans, the mouse model of RC tears have a unique and significant advantage due to the available large pool of transgenic and knockout mice, which serve as powerful tools in defining molecular mechanisms of RC diseases. Further, unlike other quadrupeds, mice use their upper extremities for feeding, cleaning, and climbing, like humans. This model will help understand the biology associated with both RC injury and repair.

We found that RC tendon-to-bone healing can be achieved as late as 6 weeks after tendon was detached with a reproducible surgical procedure. Although visible degenerative changes were seen on torn RC tendons at the time of repair, both histological and mechanical testing showed similar outcomes compared to immediate or 2-week delayed repair. This data suggests a considerable treatment window for repairing RC tendons after are transected in a mouse model. However, our histological analysis showed persistent muscle FI in the 6-week delayed repair group, with only minimal FI seen in the 2-week delayed repair group. This data suggests that this model closely mimics what is seen in successful chronic human repairs and will allow for testing of muscle-based treatment strategies to improve muscle quality.

Downhill running upper-limb gait analysis has been used to measure shoulder function after RC tears in other studies.¹ We found that gait analysis was highly reproducible and was able to demonstrate differences in tear healing, as well as improvements in function as animals recovered. Further we found reduced shoulder function was closely correlated to RC muscle FI regardless if there was a successful tendon repair (the 6-week delayed repaired group). This data suggests that RC muscle properties may be as important a factor for shoulder function as a successful tendon-to-bone healing after delayed tendon repair. This is consistent with other studies that show FI persists even after successful RC repair in clinical studies.^{6,31} Thus, since RC muscle has a relatively narrow window before undergoing fatty degeneration, prevention of RC muscle fatty degeneration may be considered an important factor when determining a proper treatment window for RC tendon repair.

Like all mouse and rat RC tear models, the SS and IS tendon can spontaneously reattach after transection with scar tissue. However, our histology and mechanical testing showed that this spontaneous reattachment with scar tissue is not a functional healing of torn tendons. The scar tissue with randomly misaligned collagen fibers had significantly weaker strength compared to surgically repaired tendons. More importantly, spontaneous healing of torn tendons did not prevent the development of muscle atrophy and FI after tendon transection. Mice with spontaneous tendon healing also had significantly impaired gait compared to animals with immediate or short-term delayed tendon repairs. Thus, a surgical repair (earlier than 6 weeks) is needed to prevent muscle atrophy/FI and to restore normal shoulder function after tendon tears in this mouse model.

We found that RC muscle weight loss and fat content, rather than tendon mechanical properties, were significantly correlated with shoulder function as accessed with gait analysis. This data suggests that healthy muscles are critical in term of maintain normal shoulder function. Muscle weight loss and FI severity may be the two predicting factors for

shoulder function recovery at the time of tendon repair. Though tendons heal well, long-term delayed RC tears did not improve muscle weight or correct muscle FI, resulting in reduced shoulder function in mice. Thus, treatments to prevent and/or reduce muscle weight loss and FI are needed to restore shoulder function after repair, which this model should help test.

Besides spontaneous healing of RC tendons with scar tissue after transection as discussed above, there are several other limitations of this model. First, our chronic repair model allows for 6 weeks of atrophy and FI, but clinically people often have tears for years prior to the development of muscle changes. However, the amount of muscle changes we see are similar in this model to what is seen in a chronic rotator cuff injury clinically, so we believe that this amount of time, while not truly a chronic injury, represents the pathophysiology seen within the muscle well. Further, we did not have a 12 week TT group, which limits direct comparisons. Second, mouse shoulder anatomy and function have differences compared to humans. Like most of other animal models, the anatomy of the shoulder joint in mice is not the exactly the same as humans. Different than human and other bipedal animals, mice are quadrupedal and thus their shoulder joints are weight bearing. However, mice RCs do share many similarities with human RC anatomy. For example, the insertion sites of SS and IS muscles on the humerus in mice is similar to those in humans. Mice also use these SS muscles to lift arms above the shoulder for tasks including climbing and feeding. Third, the RC repair technique used in mouse model is different than that used clinically. Due to the small size of mouse humeral head, it is technically difficult to place anchors as is done in clinical cuff repairs. Thus, we sutured torn tendons directly to the humeral head with a 7–0 suture in this model, closely resembling a more traditional open repair. Fourth, shoulder function measured in this model is limited to gait analysis. Studies such as active shoulder range of motion or other shoulder functional analysis used in RC tear patients are impossible to be used on mice. Thus, we used forced running gait analysis as the major outcome for shoulder function in this model. Our data showed that gait analysis was highly reproducible and correlated well with RC muscle atrophy and FI. We will consider direct measurement of SS and IS muscle contractility in future studies but was beyond the scope of this study. Further, gait analysis allowed for sequential study of the same animal, limiting the number of animals needed for this study.

In conclusion, we developed a novel, reproducible, clinically relevant mouse model of delayed RC tendon repair. This model will allow for the study of cellular and molecular changes after RC repair, the use of genetically manipulated animals to study these changes, and an avenue to study pharmacologic and cellular therapies to improve healing in chronic RC injury.

Supplementary Material

Refer to Web version on PubMed Central for supplementary material.

ACKNOWLEDGEMENTS:

We thank Ms. Mengyao Liu (UCSF) and Ms. Kunqi Jiang (Central South University, China) for their assistance in RT-PCR and data analysis. We also thank Dr. Jeffrey Lotz (UCSF) for his advice in tendon mechanical testing.

SOURCE OF FUNDING:

This work was supported by VA BLR&D Merit review grant (1 I01 BX002680-01A2) (PI: Kim) and a pilot research grant from UCSF Core Center for Musculoskeletal Biology and Medicine (NIH 1P30AR066262-01) (PI: Feeley). Zili Wang was supported by the China Scholarship Council to study at the University of California, San Francisco.

REFERENCES:

1. Archambault JM, Jelinsky SA, Lake SP, Hill AA, Glaser DL, Soslowsky LJ. Rat supraspinatus tendon expresses cartilage markers with overuse. *J Orthop Res.* 2007;25(5):617–24. [PubMed: 17318892]
2. Bell R, Taub P, Cagle P, Flatow EL, Andarawis-Puri N. Development of a mouse model of supraspinatus tendon insertion site healing. *J Orthop Res.* 2015;33(1):25–32. [PubMed: 25231092]
3. Chaudhury S, Dines JS, Delos D, Warren RF, Voigt C, Rodeo SA. Role of fatty infiltration in the pathophysiology and outcomes of rotator cuff tears. *Arthritis Care Res (Hoboken).* 2012;64(1):76–82. [PubMed: 21770040]
4. Cho E, Zhang Y, Pruznak A, Kim HM. Effect of tamoxifen on fatty degeneration and atrophy of rotator cuff muscles in chronic rotator cuff tear: An animal model study. *J Orthop Res.* 2015;33(12):1846–53. [PubMed: 26121952]
5. Cofield RH, Parvizi J, Hoffmeyer PJ, Lanzer WL, Ilstrup DM, Rowland CM. Surgical repair of chronic rotator cuff tears. A prospective long-term study. *J Bone Joint Surg Am.* 2001;83-a(1):71–7.
6. Collin P, Kempf JF, Mole D, Meyer N, Agout C, Saffarini M, Godenéche A, Société Française de Chirurgie Orthopédique et Traumatologique (SoFCOT). Ten-Year Multicenter Clinical and MRI Evaluation of Isolated Supraspinatus Repairs. *J Bone Joint Surg Am.* 2017;99(16):1355–64. [PubMed: 28816895]
7. Connizzo BK, Sarver JJ, Han L, Soslowsky LJ. In situ fibril stretch and sliding is location-dependent in mouse supraspinatus tendons. *J Biomech.* 2014;47(16):3794–8. [PubMed: 25468300]
8. Coulthard P, Pleuvry BJ, Brewster M, Wilson KL, Macfarlane TV. Gait analysis as an objective measure in a chronic pain model. *J Neurosci Methods.* 2002;116(2):197–213.
9. Depres-Tremblay G, Chevrier A, Snow M, Hurtig MB, Rodeo S, Buschmann MD. Rotator cuff repair: a review of surgical techniques, animal models, and new technologies under development. *J Shoulder Elbow Surg.* 2016;25(12):2078–85. [PubMed: 27554609]
10. Eliasberg CD, Dar A, Jensen AR, Murray IR, Hardy WR, Kowalski TJ, Garagozlo CA, Natsuhara KM, Khan AZ, McBride OJ, Cha PI, Kelley BV, Evseenko D, Feeley BT, McAllister DR, Péault B, Petrigliano FA. Perivascular Stem Cells Diminish Muscle Atrophy Following Massive Rotator Cuff Tears in a Small Animal Model. *J Bone Joint Surg Am.* 2017;99(4):331–41. [PubMed: 28196035]
11. Gerber C, Fuchs B, Hodler J. The results of repair of massive tears of the rotator cuff. *J Bone Joint Surg Am.* 2000;82(4):505–15. [PubMed: 10761941]
12. Gerber C, Meyer DC, Schneeberger AG, Hoppeler H, von Rechenberg B. Effect of tendon release and delayed repair on the structure of the muscles of the rotator cuff: an experimental study in sheep. *J Bone Joint Surg Am.* 2004;86-a(9):1973–82.
13. Gigliotti D, Xu MC, Davidson MJ, Macdonald PB, Leiter JRS, Anderson JE. Fibrosis, low vascularity, and fewer slow fibers after rotator-cuff injury. *Muscle Nerve.* 2017;55(5):715–726. [PubMed: 27571286]
14. Gladstone JN, Bishop JY, Lo IK, Flatow EL. Fatty infiltration and atrophy of the rotator cuff do not improve after rotator cuff repair and correlate with poor functional outcome. *Am J Sports Med.* 2007;35(5):719–28. [PubMed: 17337727]
15. Itoigawa Y, Kishimoto KN, Sano H, Kaneko K, Itoi E. Molecular mechanism of fatty degeneration in rotator cuff muscle with tendon rupture. *J Orthop Res.* 2011;29(6):861–6.
16. Kanazawa T, Gotoh M, Ohta K, Honda H, Ohzono H, Shimokobe H, Shiba N, Nakamura K. Histomorphometric and ultrastructural analysis of the tendon-bone interface after rotator cuff repair in a rat model. *Sci Rep.* 2016;6:33800. [PubMed: 27647121]

17. Hampton TG, Kale A, Amende I, Tang W, McCue S, Bhagavan HN, VanDongen CG. Gait disturbances in dystrophic hamsters. *JBiomedBiotechnol*. Epub 2011;2011:235354.
18. Klomps LV, Zomorodi N, Kim HM. Role of transplanted bone marrow cells in development of rotator cuff muscle fatty degeneration in mice. *J Shoulder Elbow Surg*. 2017;26(12):2177–2186. [PubMed: 28869071]
19. Kovacevic D, Gulotta LV, Ying L, Ehteshami JR, Deng XH, Rodeo SA. rhPDGF-BB promotes early healing in a rat rotator cuff repair model. *Clin Orthop Relat Res*. 2015;473(5):1644–54. [PubMed: 25349036]
20. Laron D, Samagh SP, Liu X, Kim HT, Feeley BT. Muscle degeneration in rotator cuff tears. *J Shoulder Elbow Surg*. 2012;21(2):164–74. [PubMed: 22244059]
21. Lebaschi A, Deng XH, Zong J, Cong GT, Carballo CB, Album ZM, Camp C, Rodeo SA. Animal models for rotator cuff repair. *Ann N Y Acad Sci*. 2016;1383(1):43–57. [PubMed: 27723933]
22. Lee KW, Lee JS, Kim YS, Shim YB, Jang JW, Lee KI. Effective healing of chronic rotator cuff injury using recombinant bone morphogenetic protein-2 coated dermal patch in vivo. *J Biomed Mater Res B Appl Biomater*. 2017;105(7):1840–6. [PubMed: 27228085]
23. Liu M, Lee C, Laron D, Zhang N, Waldorff EI, Ryaby JT, Feeley B, Liu X. Role of pulsed electromagnetic fields (PEMF) on tenocytes and myoblasts-potential application for treating rotator cuff tears. *J Orthop Res*. 2017;35(5):956–964. [PubMed: 27138553]
24. Liu X, Joshi SK, Samagh SP, Dang YX, Laron D, Lovett DH, Bodine SC, Kim HT, Feeley BT. Evaluation of Akt/mTOR activity in muscle atrophy after rotator cuff tears in a rat model. *JO rthop Res*. 2012;30(9):1440–6.
25. Liu X, Laron D, Natsuhara K, Manzano G, Kim HT, Feeley BT. A mouse model of massive rotator cuff tears. *J Bone Joint Surg Am*. 2012;94(7):e41. [PubMed: 22488625]
26. Luan T, Liu X, Easley JT, Ravishankar B, Puttlitz C, Feeley BT. Muscle atrophy and fatty infiltration after an acute rotator cuff repair in a sheep model. *Muscles Ligaments Tendons J*. 2015;5(2):106–12. [PubMed: 26261789]
27. Mall NA, Kim HM, Keener JD, Steger-May K, Teefey SA, Middleton WD, Stobbs G, Yamaguchi K. Symptomatic progression of asymptomatic rotator cuff tears: a prospective study of clinical and sonographic variables. *J Bone Joint Surg Am*. 2010;92(16):2623–33. [PubMed: 21084574]
28. Maman E, Harris C, White L, Tomlinson G, Shashank M, Boynton E. Outcome of nonoperative treatment of symptomatic rotator cuff tears monitored by magnetic resonance imaging. *J Bone Joint Surg Am*. 2009;91(8):1898–906. [PubMed: 19651947]
29. Meislin RJ, Sperling JW, Stitik TP. Persistent shoulder pain: epidemiology, pathophysiology, and diagnosis. *American journal of orthopedics (Belle Mead, NJ)*. 2005;34(12 Suppl):5–9.
30. Moosmayer S, Tariq R, Stiris M, Smith HJ. The natural history of asymptomatic rotator cuff tears: a three-year follow-up of fifty cases. *J Bone Joint Surg Am*. 2013;95(14):1249–55. [PubMed: 23864172]
31. Ohzono H, Gotoh M, Nakamura H, Honda H, Mitsui Y, Kakuma T, Okawa T, Shiba N. Effect of Preoperative Fatty Degeneration of the Rotator Cuff Muscles on the Clinical Outcome of Patients With Intact Tendons After Arthroscopic Rotator Cuff Repair of Large/Massive Cuff Tears. *Am J Sports Med*. 2017;45(13):2975–81. [PubMed: 28906128]
32. Peltz CD, Dourte LM, Kuntz AF, Sarver JJ, Kim SY, Williams GR, Soslowsky LJ. The effect of postoperative passive motion on rotator cuff healing in a rat model. *JBone Joint Surg Am*. 2009;91(10):2421–9. [PubMed: 19797578]
33. Peltz CD, Perry SM, Getz CL, Soslowsky LJ. Mechanical properties of the long-head of the biceps tendon are altered in the presence of rotator cuff tears in a rat model. *J Orthop Res*. 2009;27(3):416–20. [PubMed: 18924143]
34. Potter R, Havlioglu N, Thomopoulos S. The developing shoulder has a limited capacity to recover after a short duration of neonatal paralysis. *J Biomech*. 2014;47(10):2314–20. [PubMed: 24831237]
35. Samagh SP, Kramer EJ, Melkus G, Laron D, Bodendorfer BM, Natsuhara K, Kim HT, Liu X, Feeley BT. MRI quantification of fatty infiltration and muscle atrophy in a mouse model of rotator cuff tears. *J Orthop Res*. 2013;31(3):421–6. [PubMed: 22991068]

36. Urwin M, Symmons D, Allison T, Brammah T, Busby H, Roxby M, Simmons A, Williams G. Estimating the burden of musculoskeletal disorders in the community: the comparative prevalence of symptoms at different anatomical sites, and the relation to social deprivation. *Ann Rheum Dis*. 1998;57(11):649–55. [PubMed: 9924205]

Author Manuscript

Author Manuscript

Author Manuscript

Author Manuscript

Clinical Relevance:

Our novel mouse model could serve as a powerful tool to understand the pathophysiology and cellular/molecular mechanisms of RC muscle/tendon degeneration, eventually improving our treatment strategy in treating and repairing RC tears.

Author Manuscript

Author Manuscript

Author Manuscript

Author Manuscript

What is known about the subject:

The majority of existing small animal RC repair models consist of tendon transection followed by immediate repair, in which the degenerative tendon and muscle changes seen in RC tears patients are absent, which limits the clinical relevance of these models.

What this study adds to existing knowledge:

We developed a novel mouse model of delayed RC tendon repair. We evaluated tendon-to-bone healing, muscle histology, as well as shoulder function with gait analysis in mice with delayed RC tendon repairs.

Author Manuscript

Author Manuscript

Author Manuscript

Author Manuscript

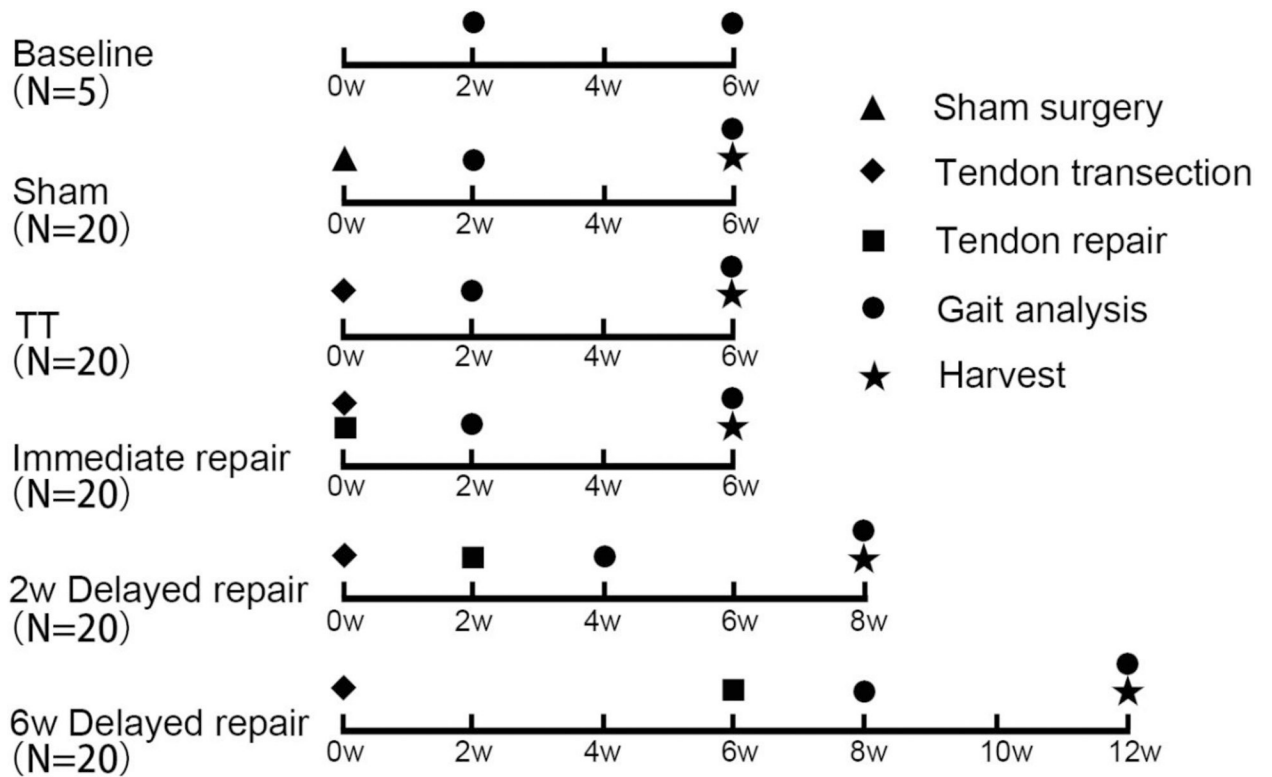


Figure 1. Flow Diagram of Experiment Design. Baseline (N=5) was served as control for gait analysis. For other 5 groups (N=20 per group), 5 mice for histological staining, 5 mice for SS tendon mechanical testing, 5 mice for IS tendon mechanical testing and 5 mice for RT-PCR analysis.

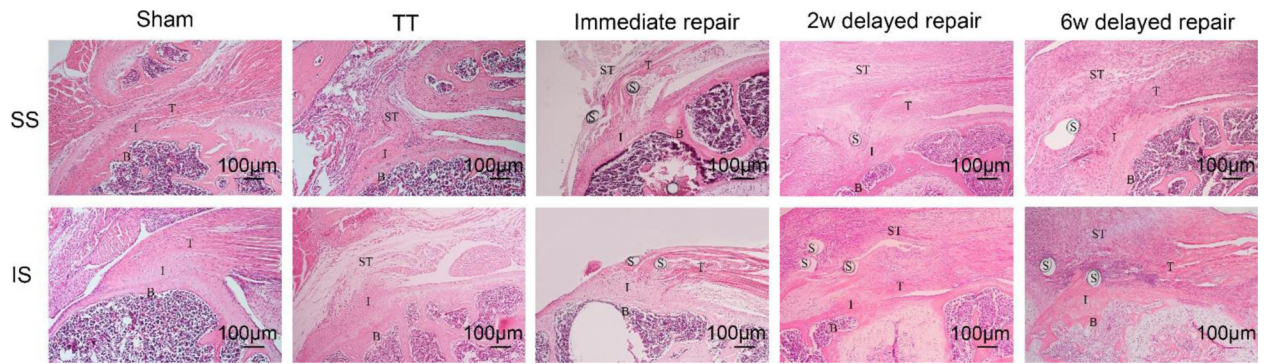


Figure 2.

H&E staining of SS tendon and IS tendon ($\times 100$). SS and IS tendons were reattached to humeral head in the three repair groups, though more synovial tissue proliferation and scar tissue was found around the tendon in the three repair groups when compared with the sham group. Only scar tissue was seen between torn tendons and humeral head in the TT group. B, bone; I, interface; T, tendon; ST, scar tissue; S, suture.

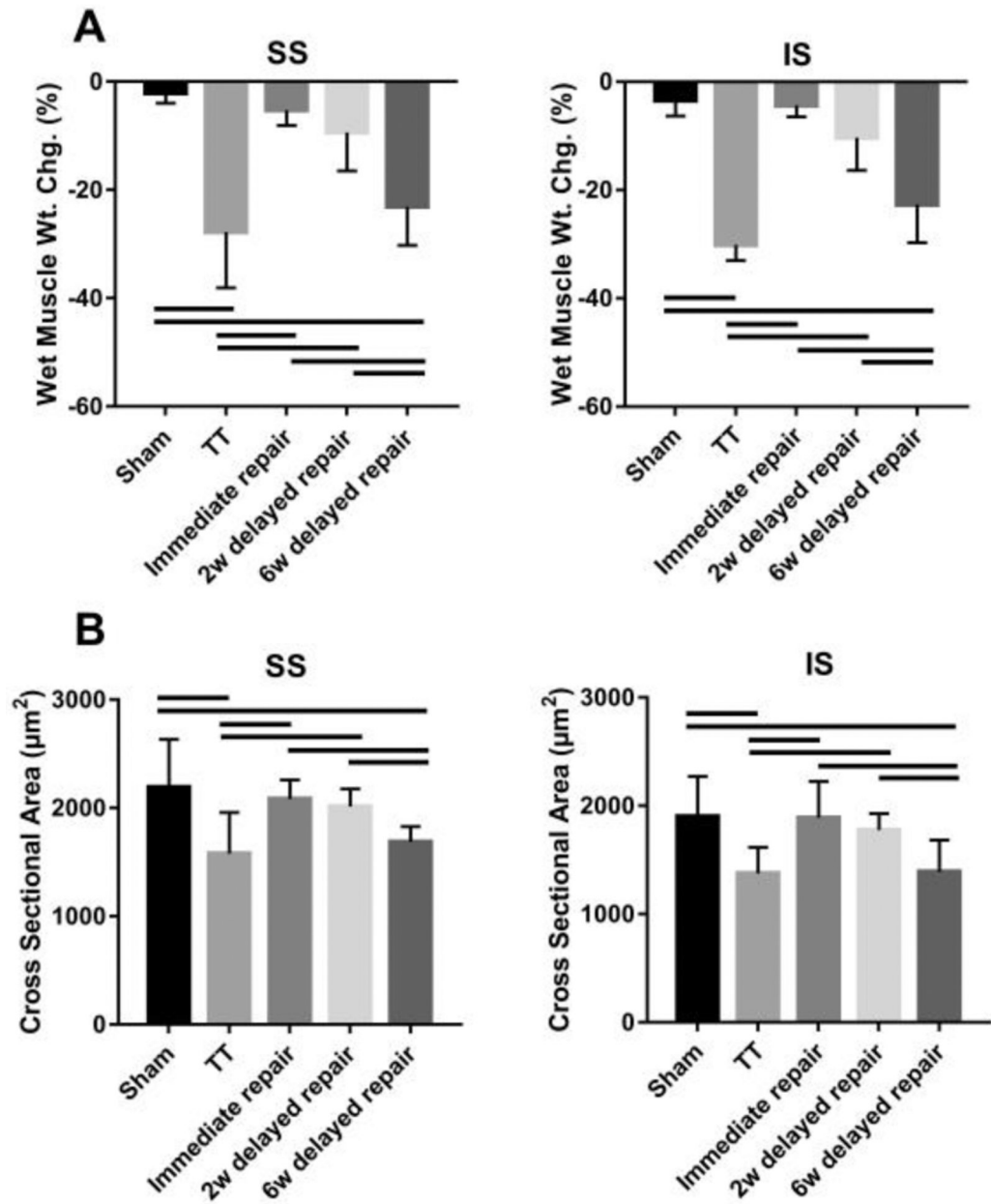


Figure 3. Percent wet muscle weight change (A) and muscle fiber cross-sectional area (B). Solid lines indicate $P < .05$. Error bars indicate the standard deviation.

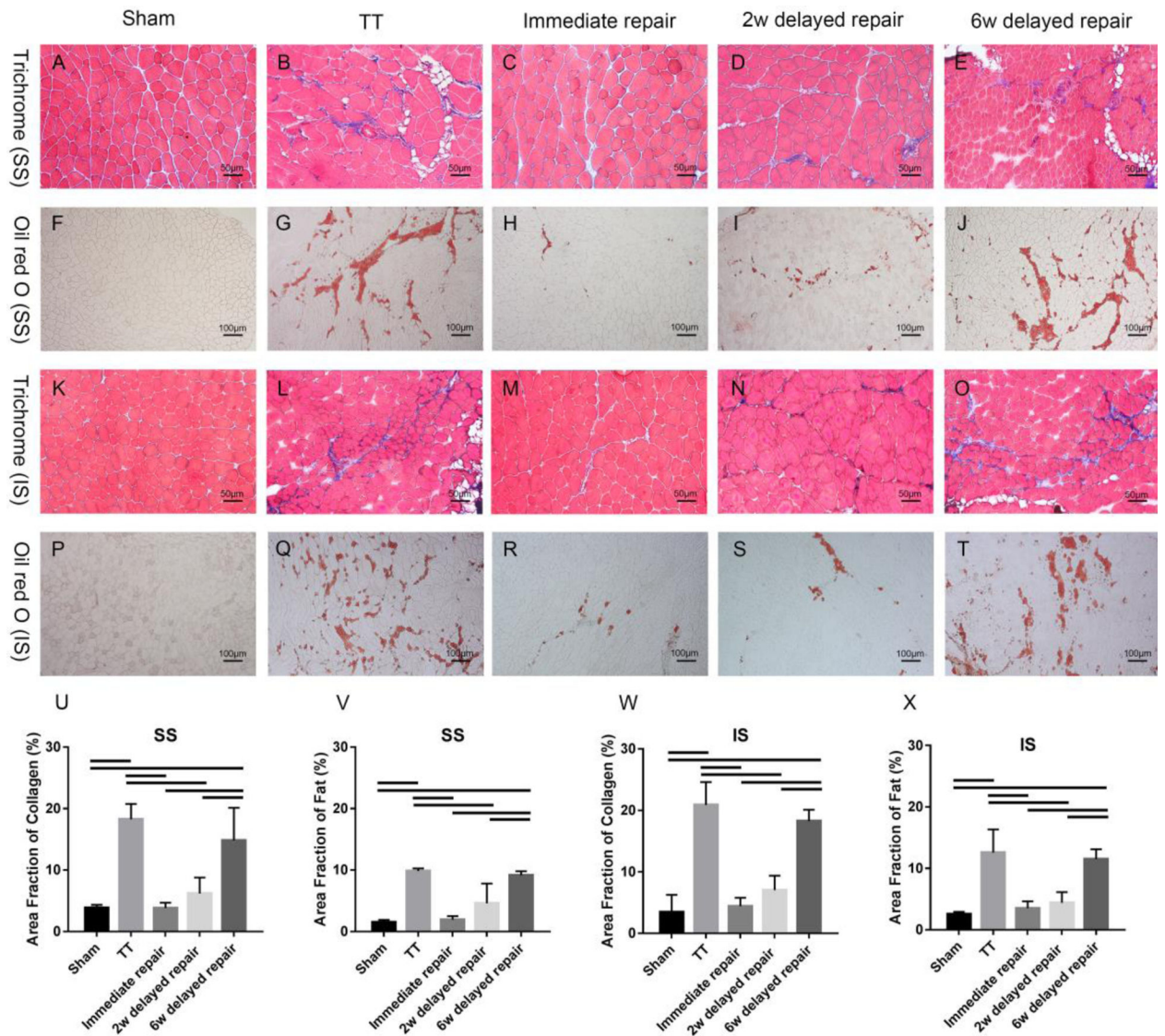


Figure 4.

Trichrome staining (A-E & K-O, $\times 200$) and Oil red O staining (F-J & P-T, $\times 100$) of SS and IS showed significant fibrosis and fatty infiltration in SS and IS muscles from the TT group and the 6 weeks delayed repair group, while only minimal fibrosis and fatty infiltration were seen in SS and IS muscles from the immediate and the 2 weeks delayed repair groups. (U-X) Significantly higher area fraction of collagen and fat were found in both SS and IS from the TT group and the 6 weeks delayed repair group. Area fraction of collagen (%) = area of collagen staining/entire sample area. Area fraction of fat (%) = area of Oil red O staining/entire sample area. solid lines indicate $P < .05$. Error bars indicate the standard deviation.

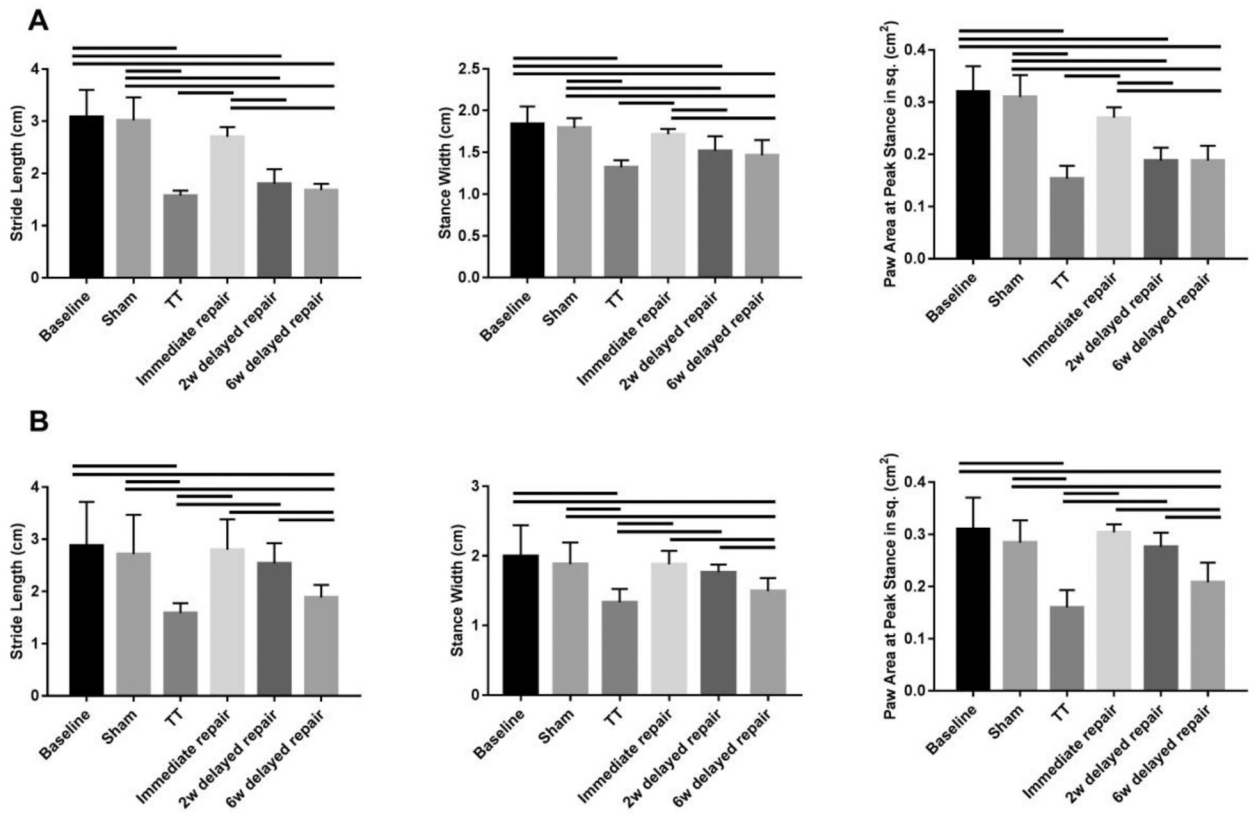


Figure 5.

Gait Analysis of injured fore limb. At 2 weeks after the last surgery, the three parameters (the stride length, stance width and paw area at the peak stance) in the TT, 2 weeks and 6 weeks delayed repair groups were significantly reduced when comparing with the baseline and sham group (A). At 6 weeks after the last surgery, the three parameters in the 2 weeks delayed repair group were recovered; however, the three parameters remained at a low level in the TT and 6 weeks delayed repair group when compared to the baseline and sham group (B). Solid lines indicate $P < .05$. Error bars indicate the standard deviation.

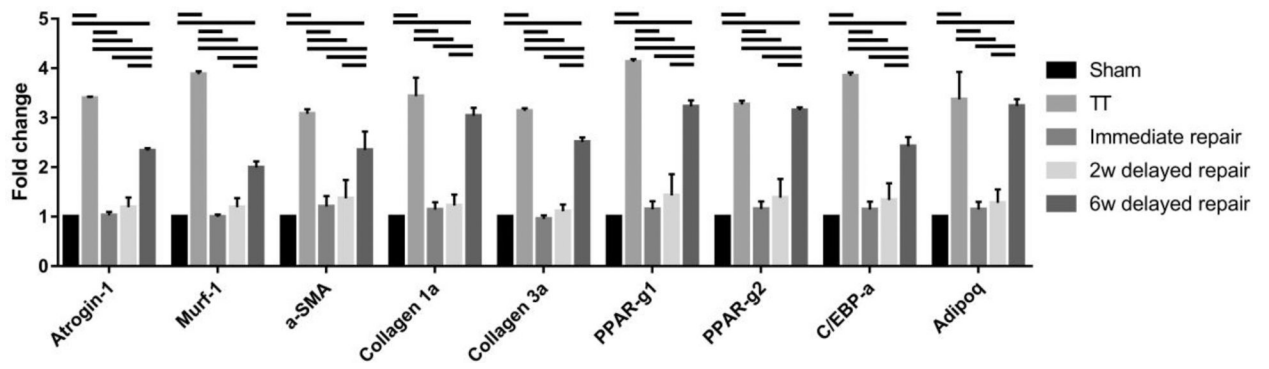


Figure 6. Atrophy, fibrosis and fatty infiltration related genes expressions. Solid lines indicate $P < .05$. Error bars indicate the standard deviation.

Table 1.Mechanical Testing of SS and IS tendons at 6 Weeks after last surgery^a

	Sham	TT	Immediate repair	2w delayed repair	6w delayed repair
Supraspinatus tendon					
Max load (N)	2.486±0.336	0.394±0.199 ^b	1.621±0.535 ^{bc}	1.334±0.467 ^{bc}	1.169±0.310 ^{bc}
Displacement at Max load (mm)	0.746±0.306	0.642±0.443	0.699±0.204	0.570±0.152	0.645±0.421
Stiffness (N/mm)	3.626±1.608	0.920±0.832 ^b	2.184±0.721 ^c	2.392±1.046 ^c	2.348±0.982 ^c
Strength (MPa)	1.753±0.651	0.278±0.157 ^b	1.828±1.488 ^c	0.938±0.480 ^c	0.751±0.340 ^{bc}
Ratio of the rupture at the tendon-muscle junction	5/5	0/5	5/5	5/5	4/5
Infraspinatus tendon					
Max load (N)	1.343±0.304	0.319±0.184 ^b	0.993±0.309 ^c	0.968±0.139 ^{bc}	0.776±0.132 ^{bc}
Displacement at Max load (mm)	0.963±0.462	1.518±0.991	1.193±1.072	0.696±0.141	0.901±0.355
Stiffness (N/mm)	2.378±0.764	0.634±0.598 ^b	1.765±0.647 ^c	1.322±0.194 ^{bc}	1.462±0.516 ^c
Strength (MPa)	0.806±0.501	0.161±0.085 ^b	0.715±0.115 ^c	0.611±0.096 ^c	0.517±0.174 ^c
Ratio of the rupture at the tendon-muscle junction	5/5	0/5	5/5	4/5	4/5

^aThe values are given as the mean and the standard deviation.^bComparing to the sham group, the difference was significant ($P < .05$).^cComparing to the TT group, the difference was significant ($P < .05$).

Table 2.

Gait Analysis Correlation to Tendon Mechanical Testing, Percent Wet Muscle Weight Change and Fat Area Fraction of the 6 Weeks Delayed Repair Group^a

Gait analysis	Mechanical testing				Percent wet muscle weight change	Fat area fraction
	Max load	Displacement	stiffness	strength		
Supraspinatus tendon						
Stride length	0.560	0.596	0.642	0.159	-0.917 ^b	-0.886 ^b
Stance Width	0.517	0.575	0.682	0.133	-0.960 ^b	-0.942 ^b
Paw Area at Peak Stance in sq.	0.620	0.737	0.863	0.397	-0.903 ^b	-0.957 ^b
Infraspinatus tendon						
Stride length	-0.289	0.454	0.368	0.282	-0.994 ^b	-0.961 ^b
Stance Width	-0.294	0.360	0.353	0.341	-0.959 ^b	-0.988 ^b
Paw Area at Peak Stance in sq.	0.073	0.099	0.602	0.484	-0.899 ^b	-0.955 ^b

^aN = 5 for each group. The values are Pearson's r of the two corresponding variables. Correlations between gait analysis and muscle weight change and fat area fraction variables were found to be significant (^b, $P < .05$)